

UNPUBLISHED

1/28/97

**Interim Report on High Level Waste Glass Model Development**

Deliverable ID MOL 108

Summary Account OL242LER

SCPB Number 8.3.5.10.

William L. Bourcier  
Glass Wasteform Task Leader

August 30, 1995.

Legacy-20

## Milestone MOL108 Interface with Controlled Design Assumption Document

The FY95 glass waste form activities provide data and models of waste form responses which are applicable to the waste package/engineered barrier system (WP/EBS) design and repository performance assessment analyses. With data and models, these analyses can evaluate WP/EBS options over a range of time-dependent boundary conditions potentially imposed on waste forms by repository environments. The results from evaluating WP/EBS options can be compared with repository functional requirements established by regulatory agencies. The primary functional requirements directly related to glass waste form rate responses are described in the Controlled Design Assumption Document (CDA) [Doc. No. B00000000-01717-4600-00032, Revision 00A, June 30, 1994] and in the Engineered Barrier Design Requirements Document (EBDRD) [YMP/CM-0024, Rev. 0, ICU-1, 21OCT94]. The regulatory requirements are stated in NRC-10 CFR60 "Disposal of High-Level Radioactive Wastes in Geologic Repositories". In the CDA, the requirements are in sections 4.2.3 (Isolate Waste) and 4.2.3.1 (Contain Waste). In the EBDRD, the requirements are provided in section 3.7 (Engineered Barrier Segment Major Components Characteristics/Requirements).

The waste form release rate responses impact evaluations and consequences of the substantially complete containment time period (SCCTP)[NRC 10CFR60.113] and the controlled release time period (CRTP)[NRC 10CFR60.113]. These two regulatory requirements are coupled because waste package failures during the SCCTP will potentially expose glass to atmospheric conditions in the repository. During this time period, glass may alter as water vapor is adsorbed to the glass surface and hydration of the glass structure takes place. Development of long-term predictive models for glass waste form degradation, the subject of this milestone report, therefore relates to these design documents.

## INTRODUCTION

This report summarizes FY95 work on developing a mechanistic model for corrosion of the borosilicate glass wasteform. Work has concentrated in three areas. The first is the incorporation of the glass model into repository performance assessment models. The glass dissolution model has been significantly simplified and several assumptions regarding repository conditions have been made in order to achieve this. This work is described in part 1 of this report.

The second topic is the application of the glass dissolution model to the unsaturated (drip) tests of HLW glass being performed at Argonne National Laboratory. These tests involve the reaction of glass in humid air while water drips onto the glass at a rate of one drop every 3.5 days. The glass dissolution model has been modified and applied to these types of test and repository conditions.

The third topic has to do with implications of recent nuclear magnetic resonance work on borosilicate glasses and the relationship between glass composition and glass durability. It has been shown that waste glasses have a microstructure that includes clustering of the boron in the glass into zones of alkali borate-rich material. This effectively depletes the matrix of the glass with respect to boron and alkalis. The overall durability of the glass is controlled by the composition of the boron-depleted matrix. Current models for composition-durability relationships (such as the hydration free energy approach) do not account for this unmixing phenomenon and should be modified to account for it. This report described a methodology for calculating glass matrix composition for clustered glasses and explains why this is important for the development of optimum glass compositions for waste containment.

Note that the types and compositions of glasses to be placed into the repository are still under evaluation and have not been precisely defined. Currently, the SRL-202 glass composition from the Savannah River Defense Waste Processing Facility (DWPF) is used as our reference glass waste form. Most of the experimental data referenced here are for SRL-202 glass.

### PART 1: INCORPORATION OF THE GLASS MODEL INTO REPOSITORY PERFORMANCE ASSESSMENT MODELS

The current glass dissolution model is complex, too complex to be incorporated into current performance assessment (PA) models of repository behavior without substantial simplification. The current model requires detailed knowledge of the evolving fluid composition. The model is incorporated into a chemical modeling code (i.e. EQ3/6; (Wolery, 1992)) which computes the solution composition along the reaction path. This information is needed in order to calculate the rate of glass alteration. However, a rigorous implementation of the glass dissolution model in PA codes requires that this detailed information on the composition of the fluid phase is available in the

PA model. This level of information and complexity is not available in current repository PA models. Simplification of the model is necessary in order for it to be interfaced into present PA codes.

### Simplification of glass dissolution model

The glass alteration rate changes as the solution composition changes, making it necessary to couple closely the evolving solution composition with glass dissolution. The rate of glass dissolution depends on the concentrations in solution of all the elements present in the surface gel layer of the dissolving glass, and also the solution pH. However, some simplifications can be made. Experimental and modeling work on borosilicate glass to date shows that the two most important solution compositional parameters which need to be considered in order to predict radionuclide release rates from glass are pH and dissolved silica concentration (temperature and reactive glass surface area must also be known). So we can restrict the feedback of solution composition to glass dissolution rate by regressing experimental rate data in terms of only these two parameters. Below we have supplied the equations and parameters needed to calculate conservative release rates of radionuclides from glass with this simplified model. We also include suggestions as to how to further simplify the model to make it appropriate for input into a first-cut comprehensive performance assessment model of a repository.

Currently, the most successful long-term dissolution models for borosilicate glass employ a rate equation consistent with transition state theory. A simplified rate equation can be given as (Bourcier, 1994):

$$R = s k \left[ 1 - \left( \frac{Q}{K} \right)^\sigma \right] + s r_l \quad (1)$$

*only used?*

- where R = alteration rate of glass (g/yr),  
s = surface area of reactive glass (m<sup>2</sup>),  
k = glass surface alteration rate constant (g/m<sup>2</sup>/yr),  
a function of temperature and pH of the solution,  
Q = concentration of dissolved silica (g/m<sup>3</sup> water),  
K = a quasi-thermodynamic solubility constant for borosilicate glass,  
here it equals the solubility of amorphous silica (g/m<sup>3</sup> water)  
σ = experimentally determined constant  
r<sub>l</sub> = long-term dissolution rate (under "silica saturated"  
conditions)

Each of these parameters must be known or estimated in order to calculate radionuclide release rates from glass. At present, the value of  $\sigma$  is not well determined based on the available experimental data. The value of  $\sigma$  is therefore set to one in this model. Suggested values for each of the other parameters are discussed below.

### *Surface Area, s*

As the molten glass cools in the melter, it undergoes fracturing. Estimates for the increase in glass surface area due to fracturing range from 2 to 100 times the uncracked surface area. A reasonable average value to use for the extent of fracturing is 25 (Baxter, 1983). The initial total glass surface area per waste package,  $A_o$ , is made up of a nominal area per glass log, number of glass logs per package,  $n$ , and a cracking factor, a multiplier on the nominal area ( $\geq 1$ , typically around 25).

$$A_o = 25 \cdot n \cdot 2\pi r_o^2 \left(1 + \frac{L_o}{r_o}\right) \quad (2)$$

where  $A_o$  = total glass surface area ( $m^2$ ),  
 $r_o$  = radius of the glass log,  
 $L_o$  = length of the glass log, and  
 $n$  = number of glass logs per waste package.

The glass log is assumed the same cylindrical shape with a constant length to radius ratio,  $L_o/r_o$ , during the dissolution process. Assuming the glass retains a constant density throughout alteration, then

$$A_1 = A_o \left(\frac{M_1}{M_o}\right)^{\frac{2}{3}} \quad (3)$$

where  $A_1$  = surface area after dissolution,  $m^2$ ,  
 $A_o$  = initial surface area,  $m^2$ ,  
 $M_1$  = glass mass after dissolution, kg,  
 $M_o$  = initial glass mass, kg.

In the bathtub water contact mode, the total surface area of the glass log is in contact with water when the container is filled. For the flow-through mode, only a fraction of surface contacts water. The wetted area depends on the groundwater flow rate. We assume the wetted area remains the same for a given water influx,  $q$ , until the total glass surface area decreases to below the initial wetted area due to the glass dissolution. Then the wetted area equals the total area until the glass completely dissolved.

### Rate Constant, $k$

The rate constant,  $k$ , has been measured over a range of pH and temperature conditions. Table 1 shows the results of  $k$  in units of  $\text{g}/\text{m}^2/\text{day}$  from flow-through experiments by (Knauss, et al., 1990). for an analog SRL-165 glass composition.

Table 1.  $\text{Log}_{10}$  glass dissolution rate in  $\text{g}/\text{m}^2/\text{day}$  (from (Knauss, et al., 1990).

| pH | T = 25°C | 50°C  | 70°C  |
|----|----------|-------|-------|
| 1  | -1.25    | 0.02  | 0.51  |
| 2  | -1.73    | -0.68 | -0.18 |
| 3  | -2.21    | -1.38 | -0.87 |
| 4  | -2.69    | -2.08 | -1.56 |
| 5  | -3.17    | -2.78 | -2.25 |
| 6  | -        | -     | -2.94 |
| 7  | -4.53    | -3.43 | -2.3  |
| 8  | -4.02    | -2.92 | -1.9  |
| 9  | -3.51    | -2.41 | -1.5  |
| 10 | -3       | -1.9  | -1.1  |
| 12 | -1.98    | -0.88 | -0.3  |

The data are plotted in Fig. 1, and the following regression relations are obtained:

$$k = 365 \times 10^m \quad (4a)$$

where  $m$  is the higher value of the following two equations:

$$m = 8.632 - \frac{2600}{T+273} - 0.65pH \quad (4b)$$

$$m = 7.268 - \frac{4550}{T+273} + 0.50pH \quad (4c)$$

where  $T$  = solution temperature ( $^{\circ}\text{C}$ ).

### Solution Chemistry, $Q$ and $K$

The major effect of groundwater chemistry on the glass dissolution rate (other than pH) is the concentration of dissolved silica. In this simple model,  $Q$  equals the concentration of dissolved silica in the water contacting the glass. The local groundwater chemistry in the vicinity of the repository will

likely be dominated by the host rocks (Wilder, 1992) and the silica concentration is therefore expected to be close to cristobalite saturation at the ambient temperature. Cristobalite is a common constituent of the host rocks at Yucca Mountain. Table 2 lists concentrations of silica in equilibrium with cristobalite at temperatures from 0 to 150°C from the thermodynamic database SUPCRT92 (Johnson, et al., 1992)

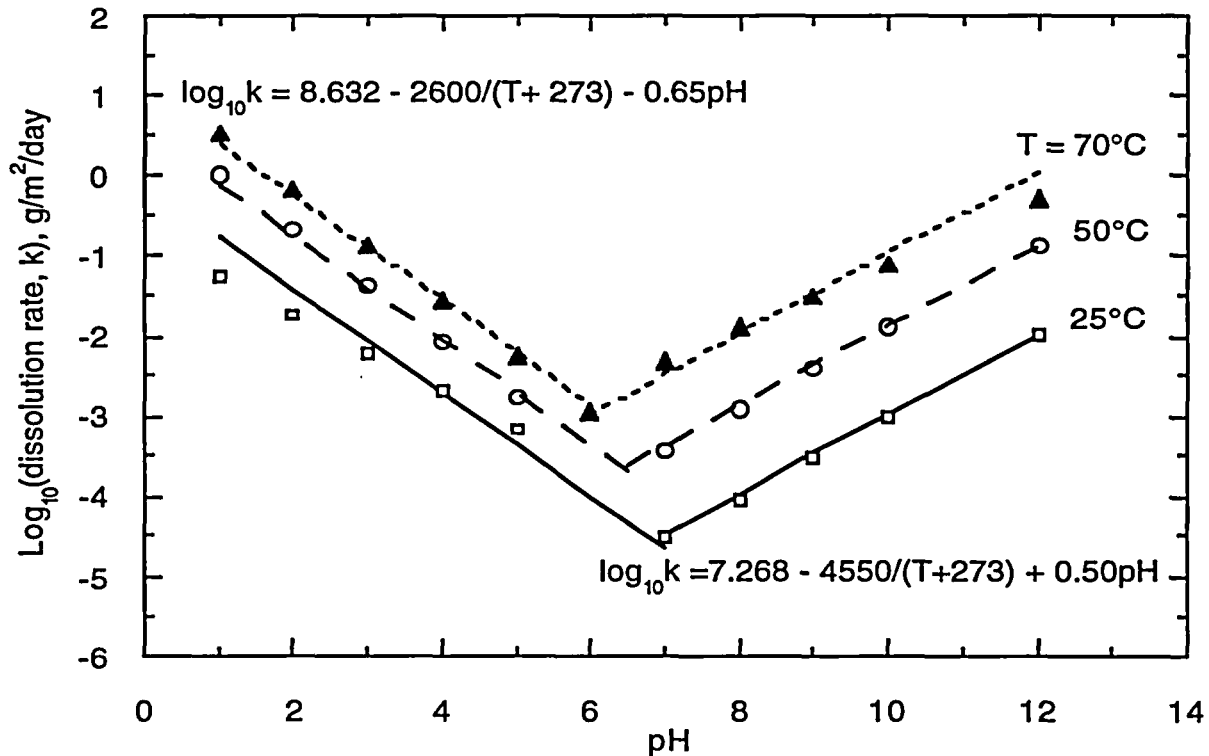


Figure 1.  $\text{Log}_{10}(\text{dissolution rate, g/m}^2/\text{day})$  versus solution pH from Knauss et al., 1990.

"K" in equation (1) for the waste glass is assumed equal to the equilibrium constant for amorphous silica in this simple model. K actually varies as a function of glass composition, but for most waste glass compositions, the experimentally determined value of K is of the same general magnitude but less than the value of K for amorphous silica. Our simplification therefore gives conservative estimates. Table 2 lists values of  $\text{log}_{10}K$  (in molality) for temperatures from 0 to 150°C. As an example, at 60°C,  $Q/K = 10^{-3.02}/10^{-2.43} = 0.26$ . The term  $(1-Q/K) = (1-0.26)$  or 0.74. The glass reaction rate therefore is about 74% of the rate under silica-free conditions.

Figure 2 shows the relation between  $Q/K$  and temperature. For a temperature between 0 and 100°C, the relation can be expressed as:

*Q from cristobalite (sat) reaction?*

$$\frac{Q}{K} = 0.128 + 0.0021T \quad (5)$$

Table 2. Cristobalite and Amorphous Silica Solubilities (from (Johnson, et al., 1992).

| T°C =            | 0     | 25    | 60    | 90    | 100   | 150   |
|------------------|-------|-------|-------|-------|-------|-------|
| Cristobalite     | -3.89 | -3.45 | -3.02 | -2.75 | -2.68 | -2.36 |
| Amorphous Silica | -2.99 | -2.71 | -2.43 | -2.26 | -2.20 | -1.98 |

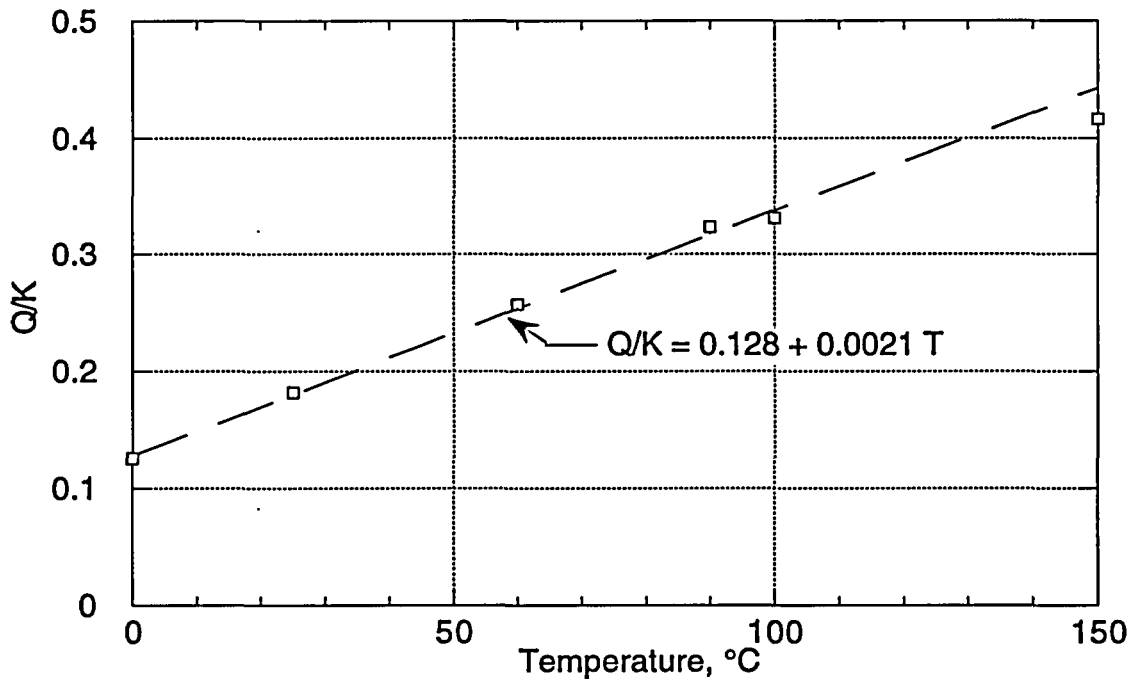


Figure 2. Relation between Q/K and temperature.

### Solution pH

Experimental studies of tuff-water interactions have shown that the pH of reacted J-13 water maintains a pH slightly higher than neutral (Knauss, et al., 1987) Therefore for anticipated repository conditions, a slightly alkaline pH of about 8 is recommended as a substitute for the lack of a more rigorous calculation of groundwater chemistry. This pH value should be used to estimate rate constants for glass dissolution from Table 1 (it should also be consistent with any data for solubility limited radionuclide concentrations which are also highly dependent on pH). Note however that glass dissolution rates and radionuclide release rates are very sensitive to pH and nothing more than a qualitative estimate of release rates is possible without a more rigorous treatment of solution chemistry in the repository performance assessment model.

$10^{-6} \text{ g/m}^2\text{-day}$   
 $10^{-8} \text{ g/m}^2\text{-day}$

*Temperature Dependence of Glass Dissolution Rate*

Experiments have shown that glass dissolution rates follow the Arrhenius relation  $\text{rate} \propto e^{-E/RT}$  where R is the gas constant, T is temperature (Kelvins) and the activation energy (E) is about 20 kcal/mole. This corresponds roughly to dissolution rate increasing by a factor of 3 for a ten degree rise in temperature. This simple rule can be used to describe the effect of temperature on glass dissolution rate if the data in Table 1 cannot be explicitly used.

*Radionuclide Content of Glass*

Table 3 lists anticipated radionuclide contents for SRL glasses. More information on glass compositions is provided in the Wasteform Characteristics Report. Conservative estimates for release rates for radionuclides from the glass wasteform are given by multiplying the glass dissolution rate (R) by the weight fraction of radionuclide in the glass from Table 3.

*Example Calculation*  $10^{-1} \text{ g/m}^2\text{-day}$   
 $10^{-5} \text{ g/m}^2\text{-day}$

What is the rate of release of  $^{235}\text{U}$  from one canister of glass at  $70^\circ\text{C}$  in cristobalite-saturated groundwater of  $\text{pH}=8$ ? The rate constant for glass dissolution at  $70^\circ\text{C}$  and  $\text{pH}=8$  is  $10^{-1.9} \text{ g/m}^2\text{/day}$ . The affinity term  $(1-Q/K)$  has a value of  $(1-10^{-2.93}/10^{-2.37})$  or 0.72. The bulk dissolution rate of glass is therefore  $0.0091 \text{ g/m}^2\text{/day}$ . Surface area for one canister is  $125 \text{ m}^2$ , so that the total rate of glass dissolution is  $1.13 \text{ g/day/canister}$ . Predicted  $^{235}\text{U}$  content of SRL waste glass is  $72.78 \text{ g/canister}$ . Total weight of glass in a canister is  $1682 \text{ kg}$  so that the weight fraction of  $^{235}\text{U}$  is  $4.3 \times 10^{-5}$ . Release rate of  $^{235}\text{U}$  is therefore  $1.13 \times 4.3 \times 10^{-5} = 4.89 \times 10^{-5} \text{ g/day}$  or  $.018 \text{ g/year}$ .

$\frac{1.25 \times 10^6 \text{ m}^2}{1.7 \times 10^6 \text{ g}} (0.7)$   
 $(56.6 \text{ m}^2/\text{g})$

Further simplification of the model can be achieved by making the following assumptions: constant pH of 8 and cristobalite saturation of the groundwater. Use Table 1 to provide the rate constant as a function of temperature at  $\text{pH} = 8$ . Use Table 2 to provide the factor that accounts for the lowering of glass dissolution rate due to dissolved silica. This provides a simple function of glass dissolution rate with temperature and no other variables need to be considered.

*Limitations of the Simplified Model*

This simplified treatment of estimating glass dissolution rates provides conservative estimates for release rates of radionuclides. It ignores solubility limits of some radioactive species (such as the actinides) and instead uses the conservative assumption that the radionuclides will be released no faster than the break down of the glass structure. This is consistent with the

measured rates of diffusion of actinides in the glass, which are negligible under repository temperatures. Experiments have shown that during glass corrosion the actinides are commonly included in alteration phases at the surface of the glass either as minor components of other phases or as phases made up predominantly of actinides. We do not take any credit for this process in this simple glass dissolution model. In order to perform accurate estimates of solubility-limited release rates, we need to know detailed information on water chemistry (pH, Eh, etc.) which demands a much more complex PA model that explicitly accounts for coupled chemical interactions between all of the repository materials (spent fuel, glass, metals, etc.).

This simple model also ignores all solution chemistry other than pH and silica concentration of the leachate. We know from a variety of experiments that species such as dissolved Mg and Fe can change glass dissolution rates by up to several orders of magnitude. Mg decreases the rate, Fe increases the rate. We do not account for effects such as these in this model. Because these effects have not yet been quantified, it is currently impossible to include them in PA models of any level of complexity.

We also ignore vapor phase alteration of the glass. If a canister containing glass is breached and humid air reaches the glass, the glass will react and form a thick alteration rind composed of hydrated glass and secondary phases. The durability of this material with respect to later contact with liquid water may be much greater or much less than the unaltered glass. We do not account for this effect here.

### Incorporation of Simplified Glass Model into YMIM

[ Much of the information presented in this section was developed jointly by Tzou-Shin Ueng, William J. O'Connell, William L. Bourcier, and Jim Gansemer. A more complete derivation of the equations which are used to predict borosilicate glass dissolution in the YMIM performance assessment code is available in Ueng et al. "Performance assessment model for a glass waste package" currently in draft form.]

Three more pieces of information are needed in order to incorporate a simple glass dissolution model into the current performance assessment model. They are:

- (1) a functional relationship between the amount of silica released into solution versus the amount which remains in solid alteration phases and layers;
- (2) a functional relationship between the pH and the amount of glass dissolved;
- (3) estimates of long-term rates determined from experimental data.

This information is necessary in order to apply the glass model to the range of hydrologic conditions from bathtub to flow-through mode using a single model. The fraction of silica released to solution is needed to compute the silica concentration in the evolving leachate. The pH is needed in order to compute the reaction rate constant for the glass during reaction progress.

**Table 3.5.1.3. Radioisotope content per HLW container for borosilicate glass from the Savannah River Site (from (Stout & Leider, 1991) Wasteform Characteristics Report, Table 6.14). Contents in grams of each isotope. Mass of glass in each canister is 1682 kilograms. Only elements with more than 1 gram per canister are reported here.**

| Isotope | g/canister | Isotope | g/canister |
|---------|------------|---------|------------|
| U-234   | .549e1     | Tc-99   | .182e3     |
| U-235   | .727e2     | Pd-107  | .286e2     |
| U-236   | .174e2     | Sn-126  | .156e2     |
| U-238   | .312e5     | Cs-135  | .863e2     |
| Np-237  | .126e2     | Cs-137  | .499e3     |
| Pu-238  | .867e2     | Ce-143  | .401e3     |
| Pu-239  | .208e3     | Ce-144  | .309e1     |
| Pu-240  | .381e2     | Nd-144  | .411e3     |
| Pu-241  | .162e2     | Pm-147  | .261e2     |
| Pu-242  | .321e1     | Sm-147  | .877e2     |
| Am-241  | .321e1     | Sm-148  | .192e2     |
| Cm-244  | .132e1     | Sm-149  | .742e1     |
| Se-79   | .243e1     | Sm-151  | .941e1     |
| Rb-87   | .996e1     | Eu-154  | .229e1     |
| Sr-90   | .343e3     | Eu-155  | .102e1     |
| Zr-93   | .444e3     |         |            |

$$\begin{aligned}
 \text{Np-237} & \quad \frac{0.126 \times 10^2}{1682 \times 10^3} = 7.5 \times 10^{-6} \\
 & \quad (3.1 \times 10^{-4}) \rightarrow \text{SF} \\
 \text{Tc-99} & \quad \frac{0.182 \times 10^3}{1682 \times 10^3} = 1.1 \times 10^{-4} \\
 & \quad (5.7 \times 10^{-4}) \rightarrow \text{SF} \\
 \text{Pu-239} & \quad \frac{0.208 \times 10^3}{1682 \times 10^3} = 1.2 \times 10^{-4} \\
 & \quad (1.1 \times 10^{-2}) \rightarrow \text{SF} \\
 \text{Am-241} & \quad \frac{0.321 \times 10}{1682 \times 10^3} = 1.9 \times 10^{-6} \\
 & \quad (4.4 \times 10^{-4}) \rightarrow \text{SF}
 \end{aligned}$$

### *Silica Distribution Between Alteration Phases And Solution*

The relationship between the amount of silica released to solution and the amount tied up in secondary phases is complex. It depends on the composition of the glass, the temperature, the pH, the composition of the starting solution, and probably other factors.

As the glass dissolves, secondary phases begin to precipitate. The types of phases which form depend on the glass composition. These phases lower the concentration of dissolved silica. Presently we cannot predict the exact phases which will precipitate for a given glass in a given fluid composition. We use data from experiments to identify the phases.

In spite of these complexities however, it is generally true that given enough time, the solution in any closed system test approaches the condition where the amount of silica released from the glass equals the amount taken up in alteration phases. This is referred to as the "silica-saturated" or "long-term" dissolution rate. This is the slowest rate at which glasses are known to react. Because high surface area to volume ratio (SA/V) test conditions act to accelerate the test, high SA/V conditions generally show behavior where "f" approaches one (silica is almost entirely in the alteration phases). "f" is the

ratio of total released silica in the alteration phases to silica in solution. Under these conditions, the PA model should predict that the glass will react at the long-term rate (see discussion of item 3 below).

The plot in Figure 3 (from Delage, et al., 1992) shows the silica fraction trapped in alteration layers versus silica concentration in solution. The relationship is one of a straight line with increasing fraction trapped in the alteration layer with increasing SA/V ratio. This is consistent with the higher SA/V tests being more advanced in terms of the extent of reaction and therefore having both higher silica concentrations in solution and higher values of "f" as the tests approach silica saturation. Unfortunately, the test conditions and raw data from which this plot was made are not published so no more interpretation is possible.

The simple linear trend reported in the Delage et al. paper should not be over interpreted. The tests are for a very restricted range of experimental conditions, in distilled water, and over a very narrow range of SA/V conditions. This simple trend cannot be reliably extrapolated to more complex conditions where fluid composition depends on other materials as well as glass, and the history of glass reaction is not known. This is because most of the initial pH increase is due to ion exchange of the outermost few microns of glass surface. After this zone is depleted of alkali, the pH increase will be reduced. In a repository with variable hydrologic regimes, evolving input fluid composition, variable temperature, and other more complex conditions, a simple linear trend between Si concentration in solution and "f" is not expected.

Some data on the value of "f" for Savannah River glasses are available. For example, data for the SRL-202 glass based on closed system tests at SA/V ratios of 10, 2000, and 20,000 m<sup>-1</sup> give f values of 0.42, 0.54, and 0.98 respectively, after about 1-2 years of reaction. SRL-202 is currently the target glass composition for the DWPF.

Based on the above discussion, it is recommended that the current PA model use a simple relationship between SA/V and "f" for the SRL-202 glass using the data in the above paragraph (and plotted below). However, the numerous conditions and limitations discussed above indicate that although the relationship provides what is a correct trend, the absolute magnitude of the value of "f" at a particular value of SA/V is only an estimate. However, this is perhaps an adequate approximation for this initial glass dissolution model. And if we limit the application to an SRL-202 glass at near-neutral to weakly alkaline pHs, the results are probably correct in a semi-quantitative sense. More experimental work and analysis of existing data are needed in order to better define whether any simple relationship between SA/V and "f" exists.

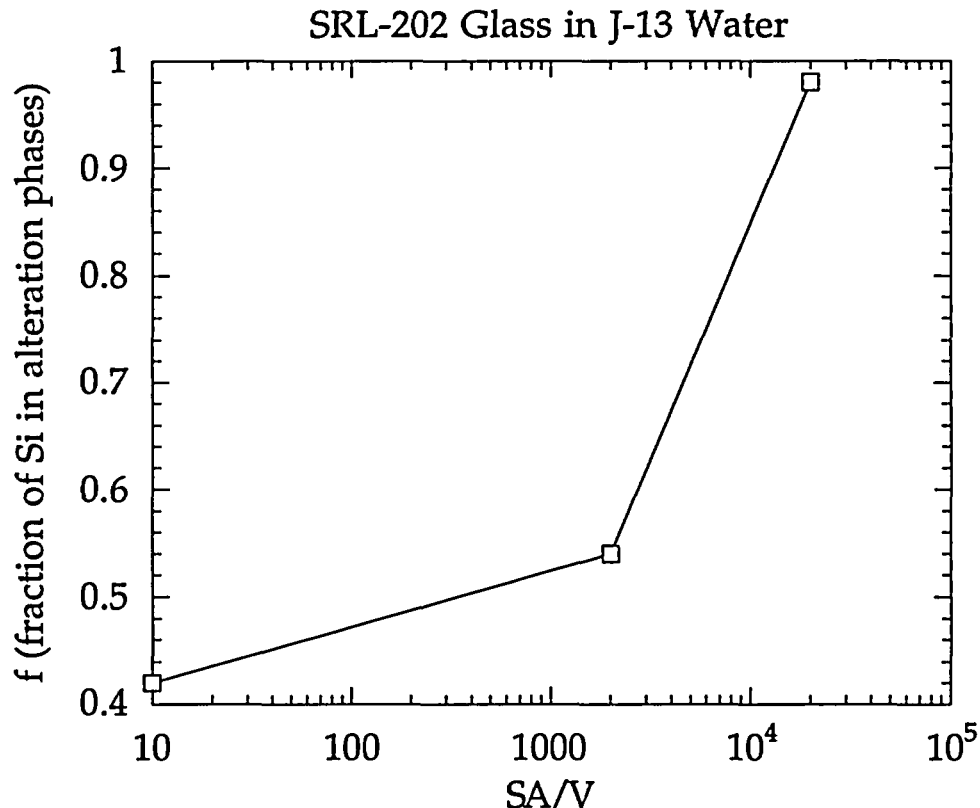


Figure 3. Experimental data for fraction of silica released from glass which is incorporated into alteration layer, as a function of surface area to volume ratio of the test.

#### *pH versus Extent of Reaction*

As glasses dissolve in closed system tests, the pH of the leachant solution increases. This is due to two effects; (1) ion exchange between cations in the glass and  $H^+$  in solution, and (2) bulk glass dissolution. Precipitation of secondary phases tends to lower the pH. For most glasses, a near-neutral unbuffered pH solution will quickly rise to pHs of between 9 and 11, depending on the alkali content of the glass (Na, Li, K) and the SA/V ratio of the test. The higher the SA/V ratio the higher the pH. The pH of the leachant quickly reaches a limiting (steady state) and nearly constant value. For tests around  $100^\circ C$ , this plateau is reached in a matter of a few days to a few weeks.

This pH effect is not important in flow-through tests. The very low effective SA/V ratios of these tests cause the ion exchange effect to be much less effective in modifying the solution pH.

An additional factor to be considered is that the solution entering the glass canister will have some initial pH and pH buffering capacity that will be greater than the buffering capacity of the distilled water used in most of the test results. This buffer capacity will oppose pH changes due to glass

dissolution and ion exchange. The change in pH will be a complex function of the flow rate, buffer capacity of the fluid, and alkali content of the glass. Again, there is also no simple relationship obvious from test results

The dominant effect in this complex situation will most likely be the ion exchange capacity of the glass. If we assume the other factors are negligible, the pH that the solution will reach can be interpreted as a simple function of SA/V ratio. At high SA/V the pH will increase to some higher constant value, at low SA/V (below about  $0.01\text{m}^{-1}$ ) the pH will not change at all.

It is impossible to consider all of these effects in the current PA model. Therefore I recommend the following simplified approach. Data for the steady-state pH for closed system tests of SRL-202 glass at 90 C are as follows:

**Table 4. Steady state pH vs. surface area to volume ratio of test.**

| Surface Area to Volume Ratio<br>( $\text{m}^{-1}$ ) | Steady State pH |
|---|-----------------|
| 10  | 9               |
| 2000  | 10.5            |
| 20,000  | 12              |

For bathtub-type hydrologic scenarios, a reasonable value for the solution pH can be estimated directly from the relationship between pH and SA/V in the table. For flow-through and intermediate hydrologic scenarios, the situation is more difficult. This is because the ion exchange process which is the dominant mechanism causing the pH to rise takes place early on in the glass-water reaction. The initial packets of reacting fluids will carry away the alkalis as high pH solutions. Later fluids will contact alkali-depleted glass which will not have nearly as great an effect on the pH of the solution. Again, because a rigorous analysis is not possible in the PA code (although it is currently something we can do in the glass submodel), I recommend extending the SA/V vs. pH relationship to the extreme end member of essentially SA/V=0 for flow-through conditions where the pH will be equal to the initial pH. A curve regressed to these data will provide a reasonable value of the pH of the reacting fluid for any given effective SA/V ratio of the system.

*Estimate of Long-Term Reaction Rate*

Experimental data showed that even when the solution is saturated with silica after a long period of time, there is still a long-term dissolution rates for several glass compositions. Because we currently do not have a mechanistic model that can predict the variation of the long-term rates with environmental parameters, an averaged experimental value must be used.

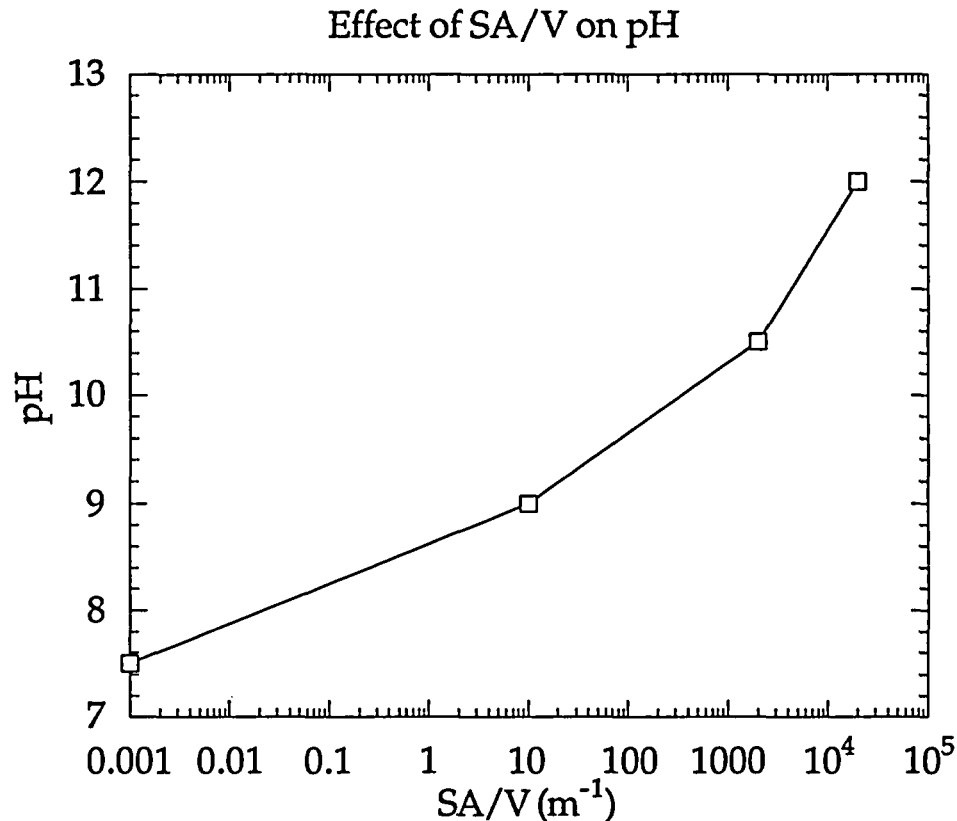


Figure 4. Steady state pH vs. surface area to volume ratio of test.

Table 5 lists measured long-term (silica saturation) dissolution rates for several glass compositions. The SRL-202 glass is the current most likely composition for glasses to be produced at WSRL and should be used for estimating glass behavior at the YMP site. Based on the data in this table, a value of 0.002 g glass/m<sup>2</sup>/day for the long-term (silica saturated) rate for SRL-202 glass is recommended.

For other temperatures, the same temperature dependency relation for the long term rate is assumed for the saturation rate. That is,

$$k_{long} \cong 2.5 \times 10^6 \text{ g / m}^2 \text{ / yr} \quad (6a)$$

$$\delta = 12 - \frac{4550}{T + 273} \quad (6b)$$

More experimental data are needed in order to improve these numbers.

Table 5. Forward and saturation rates for HLW glasses.

| Glass/Leachant                       | S/V (m <sup>-1</sup> ) | Forward Rate      | Saturation Rate     | Reference |
|--------------------------------------|------------------------|-------------------|---------------------|-----------|
| <b>Static Tests</b>                  |                        |                   |                     |           |
| PNL 76-68/DIW                        | 2000                   | 1.6               | 0.08 <sup>a</sup>   | A         |
| SRL 165/DIW                          | 2000                   | 0.80              | 0.024 <sup>a</sup>  | A         |
| EMS-11/DIW                           | 2000                   | 0.083             | 0.0016 <sup>a</sup> | A         |
| JSS-A/DIW                            | 10 <sup>b</sup>        | 1.5               | 0.0025              | B         |
| PNL 76-68/DIW                        | 10 <sup>b</sup>        | 1.8               | 0.0075              | B         |
| SRL 131/DIW                          | 10 <sup>b</sup>        | 3.0               | 0.033               | B         |
| SRL 131/J-13 <sup>c</sup>            | 10                     | 0.14              |                     | C         |
| SRL 131/J-13                         | 2000                   | 0.24              | 0.021               | C         |
| SRL 131/J-13                         | 20,000                 | 0.84              | 0.053               | C         |
| SRL 202/J-13                         | 10                     | 0.10              |                     | C         |
| SRL 202/J-13                         | 2000                   | 0.025             | 0.0016              | C         |
| SRL 202/J-13                         | 20,000                 | 0.04              | 0.0025              | C         |
| R7T7/DIW                             | 5                      | 4.9 (100°C)       |                     | D         |
| R7T7/DIW                             | 50                     |                   | 0.0083              | E         |
| R7T7/Volvic <sup>d</sup>             | 50                     |                   | 0.0133              | E         |
| R7T7/DIW                             | 400                    |                   | 0.0045              | E         |
| R7T7/Volvic                          | 400                    |                   | 0.025               | E         |
| R7T7/Volvic                          | 2000                   |                   | 0.0006              | E         |
| R7T7/Volvic                          | 8000                   |                   | 0.0006              | E         |
| R7T7/Volvic                          | 20,000                 |                   | <0.0001             | E         |
| MW/DIW                               | 1320                   | 1.1               | 0.01                | F         |
| <b>Dynamic Tests</b>                 |                        |                   |                     |           |
| SRL 202/pH 7 Buffer                  |                        | 0.28 (80°C)       |                     | G         |
| SRL 165 <sup>e</sup> /pH 10.5 Buffer |                        | 0.05 <sup>a</sup> |                     | H         |
| SRL 165 <sup>e</sup> /pH 10 Buffer   |                        | 0.08 (70°C)       |                     | I         |
| R7T7/DIW                             |                        | 1.03              |                     | J         |
| SRL 131/DIW                          |                        | 2.5               |                     | K         |

a - Estimated

b - Values determined from results of both static and dynamic tests

c - Tuff groundwater. Major components are Si(45), Na(55), HCO<sub>3</sub>-(1

d - Granite groundwater. Major components are Si(11), Ca(9.8), Na(9. ppm.

e - Analog glass without iron.

(see (Cunnane, 1993) volume 2, page 75, for references)

Clearly, a simplified model of glass dissolution will have numerous conditions and limitations that will make it unable to predict accurate behavior outside a clearly defined and restricted set of conditions. A single mechanistic model that covers the range of hydrologic conditions from flow-through to bathtub-type scenarios does not currently exist. However, by making several simplifying assumptions, we have developed a simple model based on mechanistic glass dissolution reaction that can be used to predict both closed-system (bathtub) type conditions and flow-through test conditions with some ability to model hydrologic condition between those two end member scenarios.

#### *Future Modeling Work Related to Performance Assessment Calculations*

The goal of the glass task has been to develop a mechanistic model at the level where the model predicts an alteration/dissolution rate given localized conditions. That is, for any spot on the glass, a packet of water with some composition and temperature will cause the glass to react at some rate, and produce some set of alteration products. Integration of this localized process would provide the behavior on a repository scale. Parameters like SA/V ratio and  $f$  (fraction of Si in precipitates) are not input parameters but instead are derived parameters based on the fundamental mechanisms incorporated in the glass reaction model. Although this amount of detail will not be appropriate for PA models, we need some way to progress from the fundamental model to the simplified model which involves some other approach than the purely empirical approach used in this memo. The work described here in meant to be a first step in making this connection.

For the future, we clearly need more work in two areas: (1) generating models for long-term glass dissolution rates as a function of environmental conditions, and (2) an improved approach towards transforming our mechanistic models into simplified but mechanistically based PA input.

#### Glass Release From A Waste Package

Two water contact modes, flow-through and bathtub, are considered here. In the flow-through mode, as shown in Fig. 3, we assume the water flowing down the side of a waste glass log without mixing, and keeping a surface area,  $s$ , wet. In the bathtub mode, the waste package develops a breach and water flows in and fills up over time and eventually overflows as illustrated in Fig. 4. The water inside the container is assumed well mixed.

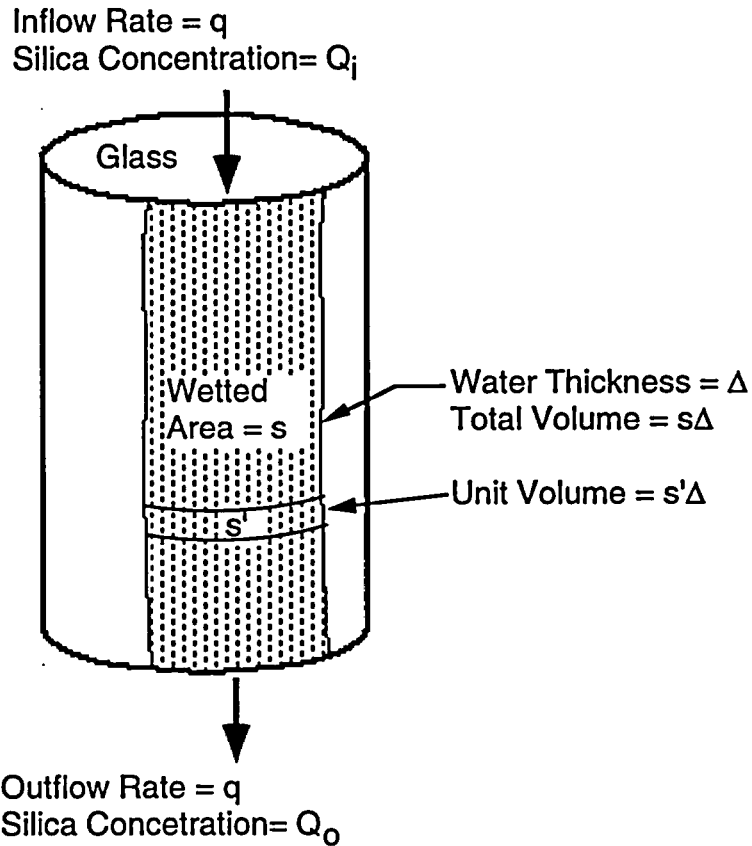


Figure 5. Flow-through Water Contact Mode

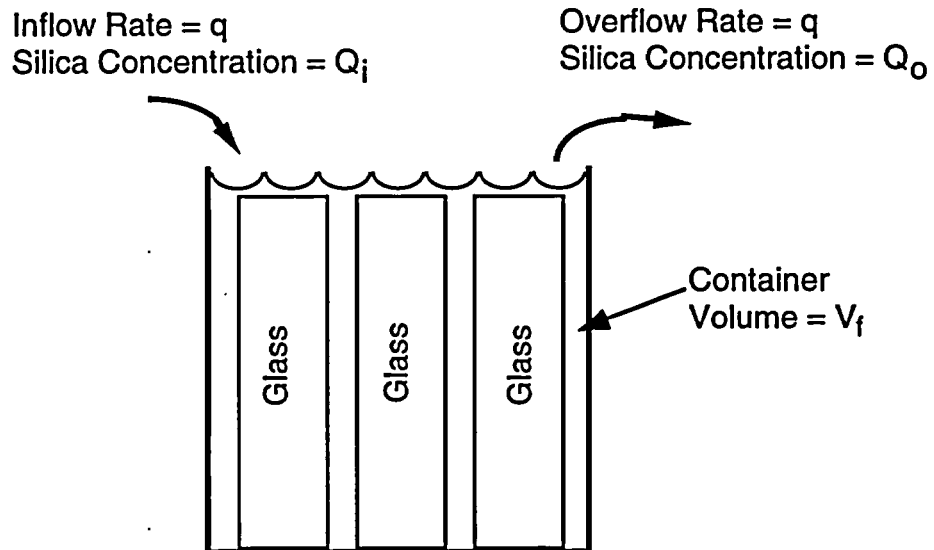


Figure 6. Bathtub Water Contact Mode

Equation (1) predicts that the dissolution rate will slow down as the dissolution adds to the silica in solution. Silica ( $\text{SiO}_2$ ) is one of the components of glass waste. For example, the DWPF glass contains about 50 wt% of silica (Cunnane, 1993). After water flows inside the waste package, the

change of silica concentration in the solution comes from the dissolution of silica released from the glass during alteration process. As the glass dissolves, secondary phases begin to precipitate. A fraction of the silica,  $f_p$ , contained in the glass will be trapped in the secondary phases. That is, only  $(1 - f_p)$  of silica in altered glass actually dissolves in the solution. The value of  $f_p$  increases with increasing surface area to volume ratio and silica concentration in solution. Since there is not sufficient data for consideration of the change of  $f_p$ , a constant intermediate value of  $f_p$  is assumed in our model.

On the other hand, the dissolution rate will change because of changes of pH in the solution. However, the change in pH will be a complex function of the flow rate, buffer capacity of the fluid, and alkali content of the glass. There is insufficient data to obtain a relationship for the change of pH due to the dissolution of glass. Therefore, only the initial pH value of the inflow groundwater is used in the calculation. This is probably true for the flow-through mode with a high flow rate.

### *Flow-through Mode*

The area of the glass log wetted by water,  $s$ , is usually unknown in the flow-through water contact mode. It is to be determined within the model for in-package hydrology. A larger wetted area generally produces a larger release. For glass, the larger area produces a slowdown of alteration rate due to the silica in solution nearing saturation. The two effects oppose each other. Also there is a long-term alteration rate which provides a minimum on the rate factor. The net release rate which results as a consequence of these three factors must be evaluated with the numerical model. It cannot be predicted in a simple way.

With a thickness of the water film on the glass of  $\Delta$ , the volume of water covering the glass is  $s\Delta$ . When groundwater of a flow rate of  $q$  covers a portion of surface area as shown in Fig. 5, the time for the water to flow in and out of the package is  $t_{in} = s\Delta/q$ . As the water proceeds downward, the silica increases and the reaction rate slows down. For a steady state flow condition, the glass dissolution condition can be considered like a unit volume of water ( $s\Delta$ ) contacting the glass for a duration of  $t_{in}$ . The increase of silica concentration during a time interval,  $dt$ ,

$$dQ = \frac{s'kf_{si}(1-f_p)}{s'\Delta} \left(1 - \frac{Q}{K}\right) dt \quad (7)$$

where  $f_{si}$  = fraction of silica in glass. Therefore,

$$-\ln\left(1 - \frac{Q}{K}\right) = \frac{kf_{si}(1-f_p)t}{K\Delta} + C \quad (8)$$

where C is a constant depending on the initial conditions. If the silica concentration of incoming groundwater is  $Q_i$ , and that of outgoing is  $Q_o$  after a duration of  $t_{in}$ , then

$$Q_o - Q_i = K \left(1 - \frac{Q_i}{K}\right) [1 - \exp(-\alpha)] \quad (9)$$

where  $\alpha = f_{si}(1 - f_p) \frac{ks}{Kq}$ .

Let  $\beta = ks/Kq$ , then we can see that a high water refresh rate gives a low value of  $\beta$ . When  $\beta$  is high the system approaches a saturated condition. Also  $f_p$  starts changing toward high values but there are not very precise data for  $f_p$ . We use the intermediate value of 0.5.

Since only a fraction of silica,  $f_{si}(1 - f_p)$ , in the waste glass dissolves in the solution, the total mass of dissolved glass per unit volume of outgoing water should be

$$G_o = \frac{Q_o - Q_i}{f_{si}(1 - f_p)} \quad (10)$$

The dissolution rate (g/yr) from the whole waste glass in the waste package for the flow-through water contact mode is,

$$R = qG_o = \frac{q(Q_o - Q_i)}{f_{si}(1 - f_p)} = \frac{qK}{f_{si}(1 - f_p)} \left(1 - \frac{Q_i}{K}\right) [1 - \exp(-\alpha)] \quad (11)$$

According to data in Table 2,  $K$  (g/m<sup>3</sup>) can be expressed as:

$$K = 6.0 \times 10^{-5} + 1.90 \times 10^{-6} T + 1.25 \times 10^{-8} T^2 \quad (12)$$

When the silica concentration is very near its saturation limit, then a long-term rate applies. The mass of glass dissolved in a unit volume of water in a time interval,  $dt$ , is

$$dG = \frac{s k_{long}}{s \Delta} dt \quad (13)$$

The dissolved glass mass per unit volume of water exiting the waste package is:

$$G_o = \frac{k_{long} t_{in}}{\Delta} = \frac{s k_{long}}{q} \quad (14)$$

Thus,

$$R = qG_o = sk_{long} \quad (15)$$

### Bathtub Mode

During filling of the container, we assume that the fraction of wetted area increases in proportion to the fraction of the filled volume in the container as shown in Fig. 4. That is,

$$\frac{A(t)}{V(t)} = \frac{s}{V_f} \quad (16)$$

where  $A(t)$  = wetted surface area of glass at time  $t$ ,  
 $V(t)$  = volume of water in the container at time  $t$  equal to  $qt$ ,  
 $s$  = total surface area of glass in the waste package,  
 $V_f$  = water volume of bathtub when filled.

The increment of silica concentration during a time interval before overflowing is:

$$dQ = \frac{A(t)}{V(t)} kf_{si}(1-f_p) \left(1 - \frac{Q}{K}\right) dt = \frac{s}{V_f} kf_{si}(1-f_p) \left(1 - \frac{Q}{K}\right) dt \quad (17)$$

The surface area of the glass logs decreases as the glass dissolves. Conservatively, we can assume the surface area remains the initial value during the filling period. Then,

$$-\ln\left(1 - \frac{Q}{K}\right) = \frac{s}{KV_f} kf_{si}(1-f_p)t + C_1 \quad (18)$$

where  $C_1$  is a constant depending on the initial conditions. The time for filling up the container is  $t_f = V_f/q$ . If the silica concentration of incoming groundwater is  $Q_i$ , and that at the time of overflow is  $Q_f$ , then

$$Q_f - Q_i = K \left(1 - \frac{Q_i}{K}\right) \left[1 - \exp\left(-\frac{skf_{si}(1-f_p)t_f}{KV_f}\right)\right] = K \left(1 - \frac{Q_i}{K}\right) [1 - \exp(-\alpha)] \quad (19)$$

where  $\alpha = f_{si}(1-f_p) \frac{ks}{Kq}$ .

To estimate the mass of glass dissolved during filling, we consider the possible maximum increase of silica concentration of the solution inside the container:

$$(Q_f - Q_i)_{\max} = K \left( 1 - \frac{Q_i}{K} \right) \quad (20)$$

According to Table 2, the silica concentration increase at 90°C is 0.000225 g/m<sup>3</sup>. For four glass logs of 0.3 m in radius and 2.2 m in length inside a container with a radius of 0.80 m and a length of 3.76 m, the bathtub volume,  $V_f$ , is 5.072 m<sup>3</sup>. Assuming  $f_{si} = 0.45$  and  $f_p = 0.5$ , we obtain the mass of dissolved glass during filling =  $0.000225 \times 5.072 / (0.45 \times 0.5) = 0.0051$  g. This loss of mass is negligible compared with the initial mass of glass logs of 6720 kg. Therefore, the assumption of constant surface area of glass is appropriate during the filling period.

After filling, i.e.,  $t > t_f$ , the change of silica in the water inside the container will be:

$$V_f dQ = \left[ skf_{si}(1 - f_p) \left( 1 - \frac{Q}{K} \right) - (Q - Q_i)q \right] dt = [(\alpha K + Q_i) - (\alpha + 1)Q] q dt \quad (21)$$

The loss of mass of glass long time after filling can be significant. To deal with changes of surface area resulting from the dissolved mass of the glass logs, calculations can be performed with time steps. Again, the surface area can be conservatively assumed constant as the initial value. Then, solving the differential equation with the boundary conditions at the time of overfilling, we obtain

$$Q_o - Q_i = \frac{\alpha K}{\alpha + 1} \left( 1 + \frac{Q_i}{K} \right) [1 - \exp(-\tau)] + (Q_f - Q_i) \exp(-\tau) \quad (22)$$

where  $\tau = \frac{(1 + \alpha)(t - t_f)}{t_f}$ . For a steady state when  $t \rightarrow \infty$ ,  $\exp(-\tau) \rightarrow 0$ , then

$$Q_o - Q_i = \frac{\alpha K}{\alpha + 1} \left( 1 - \frac{Q_i}{K} \right) \quad (23)$$

The release rate (g/yr) of the waste glass out from the waste package for the bathtub mode is,

$$R = \frac{q(Q_o - Q_i)}{f_{si}(1 - f_p)} \quad (24)$$

For the long-term silica-saturated condition,

$$R = s k_{long} \quad (25)$$

## *Radionuclide Release Calculations*

This glass alteration model has been implemented in the LLNL's performance assessment code, "Yucca Mountain Integrating Model (YMIM)," (Lamont & Gansemer, 1994). We assume that the radionuclides, regardless of their solubility, will be freed from the glass, and released either in the solution or in a colloidal form, as fast as the glass structure breaks down. This is a conservative estimate of release rate, especially for some solubility limited species, such as the actinides.

YMIM considers the water contact as a flow-through mode, i.e., there is no accumulation of water inside the container. In batch tests, the alteration rate near the end of the test and the rate of approaching a long-term value depend on the volume to surface area ratio ( $m$ ), i.e., how much initial water is available covering each unit of the glass surface area. In the steady flow-through case, the resulting alteration rate depends on the ratio  $q/s$  ( $m/y$ ), i.e., on how much incoming ambient water is provided for each wetted unit of the glass surface area (per year). A ratio  $q/s$  of  $10^{-4}$  ( $m/y$ ) is on the low side, and is recommended as a relatively conservative value because it provides a large area  $s$  for a given water influx  $q$ . This value arises, for example, from an influx of  $10^{-3}$   $m^3/y$  of water and a wetted area of  $10$   $m^2$ , or from an influx of  $10^{-4}$   $m^3/y$  of water and a wetted area of  $1$   $m^2$ . To examine the effect of a smaller wetted area, one would input a smaller value of  $s$ , smaller by one to three orders of magnitude.

Experimental studies of tuff-water interactions have shown that the pH of reacted J-13 water maintains a pH slightly higher than neutral (Knauss, et al., 1987). Therefore for anticipated repository conditions, slightly alkaline pH of 8 is suggested as a substitute for the lack of any more rigorous calculation of groundwater chemistry.

Calculations of the radionuclide releases from a waste package were conducted for two aerial thermal power densities, 57 and 114 kW/acre for a drift emplacement with backfill at 75 years. The temperature histories of waste package container and glass logs for these two thermal loadings are given in Figures 7 and 8. The input parameters for the YMIM calculations are given in Table 6. The radionuclide contents of the glass logs are given in Table 3. Note that the HLW package will contain four logs. The radionuclide inventory per package is therefore the value in Table 3 multiplied by four.

Figure 7 shows the calculated cumulative releases of the tracked radionuclides from the waste package for wetted areas of  $0.25$   $m^2$  and  $25$   $m^2$ .

Table 6. Input Parameters Used by YMIM for HLW Glass

---

**Geochemistry conditions**

pH = 8

Carbonate concentration = 0.002 mole/liter

**Hydrology conditions**

Volume of water entering failed container,  $q = 2.5$  liters/year

**Container degradation parameters**

Outer container wall thickness = 0.95 cm

Inner container wall thickness = 10.0 cm

Fraction of containers failing by defect = 0.02

Mean of exponential defective failure distribution = 100 years

*general aqueous corrosion*

follows an Arrhenius relationship. Parameters fit from the following data:

General aqueous corrosion rate at 20°C = 0.012 mm/year

General aqueous corrosion rate at 80°C = 0.038 mm/year

*stochastic pitting model* parameters:

70°C pitting increment: lognormal distribution

mean value = 0.03 mm/year

5th percentile value = 0.003 mm/year

95th percentile value = 0.3 mm/year

100°C pitting increment: 100x sampled 70°C pitting increment value

Expected number of pit growths per year = 0.033

**Glass characteristics**

Initial glass density,  $\rho_o = 2.7$  g/cm<sup>3</sup>,

Initial radius of glass logs,  $r_o = 0.3$  m,

Initial length of glass logs,  $L_o = 2.2$  m,

Mass fraction of silica in glass,  $f_{si} = 0.45$ ,

Long term alteration rate of glass,  $k_{long} = 0.73$  g/m<sup>2</sup>/yr,

Fraction of altered silica in precipitates and gel layer,  $f_p = 0.5$ ,

Wetted surface area of glass logs in a package,  $s = 25$  m<sup>2</sup> and 0.25 m<sup>2</sup>.

---

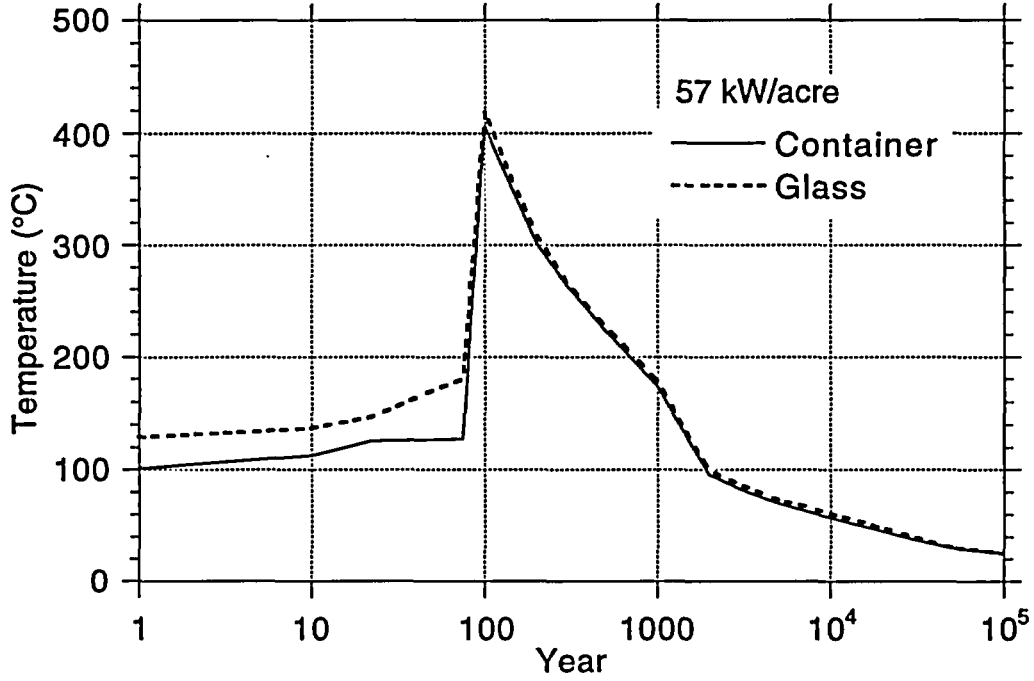


Figure 7. Temperature history for the glass logs with backfill at 75 years for thermal load of 57kW/acre.

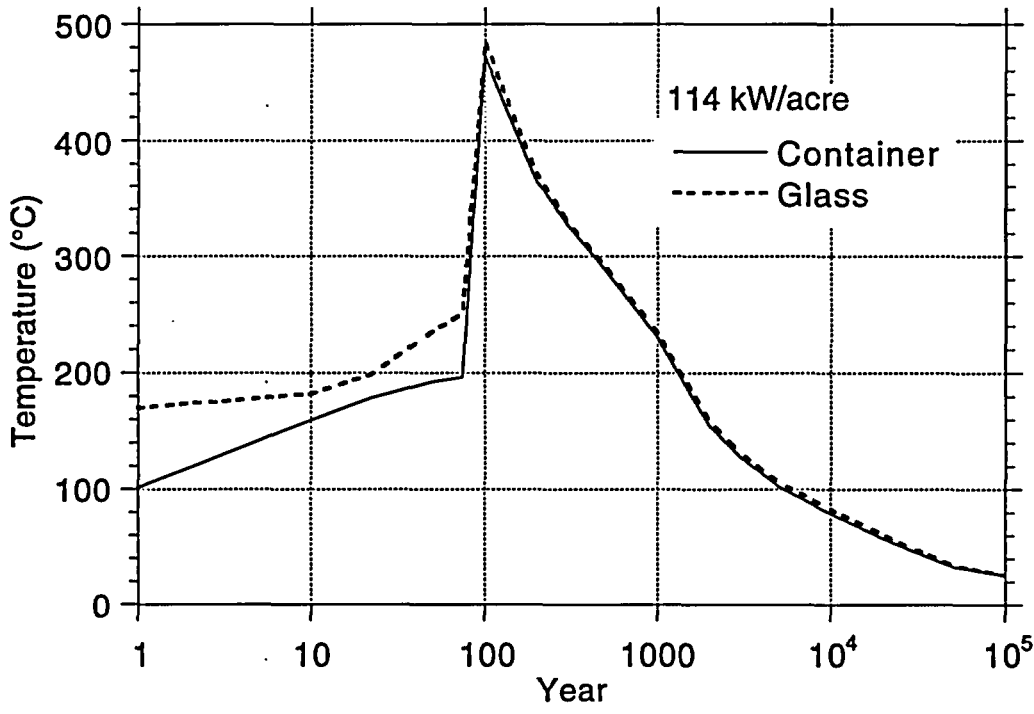


Figure 8. Temperature history for the glass logs with backfill at 75 years for thermal loading of 114kW/acre.

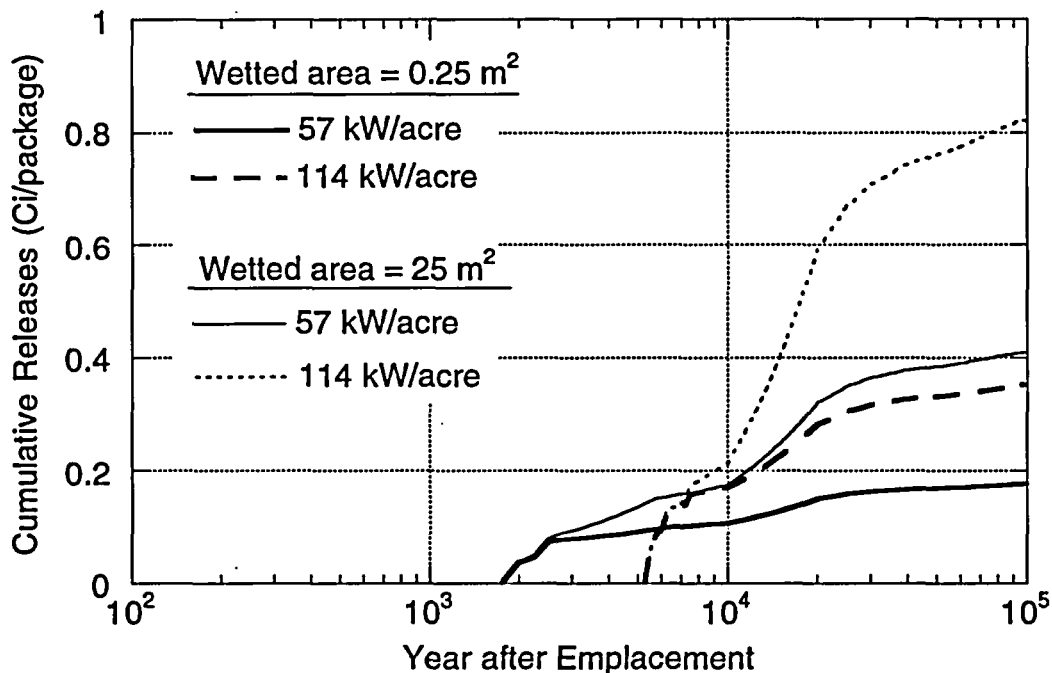


Figure 9. Cumulative release from waste package of HLW glass

## PART 2: MODELING UNSATURATED (DRIP) TESTS

A likely repository scenario for the Yucca Mountain potential repository site is that of exposure of the waste forms to dripping water. For that reason, an unsaturated test methodology was developed in order to be able to predict glass wastefrom performance in this type of environment (Bates & Gerding, 1989). These tests had previously not been analyzed using the models developed to understand and predict glass behavior in saturated environments.

We used our glass model and the rock-centered reaction mode of the React code (Bethke, 1992) to simulate the response of the SRL-202 glass to the unsaturated test conditions. React was used rather than EQ3/6 because React has the capability to model the rock-centered open system. The reference frame for this type of simulation is that of the rock which has water flowing by and reacting with it. The open-system reference frame of EQ3/6 is that of a fluid-centered system. The simulation follows a packet of water as it flows through rock. The rock-centered system was thought to be more appropriate for the drip tests. Note that neither type of simulation is rigorously correct. A code which

couples flow and chemistry is needed. We plan to employ one or more of the reactive transport codes (such as 1D-React) currently being used to investigate the near-field environment, to simulate glass-water reactions.

The unsaturated test consists of dripping a single drop (0.075ml) every 3.5 days on top of a glass wafer (13.5 cm<sup>2</sup>) secured in a stainless steel frame. If the water is assumed to contact the entire glass wafer the test has an effective SA/V ratio of about 18,000m<sup>-1</sup>. In the modeling, we assume that each drip contacts the entire glass surface for 3.5 days, and then is completely replaced with a new drop. In a real experiment, some of the glass probably falls off the glass surface before the 3.5 day interval is over, and the new drop probably mixes to some extent with the previous drop on the glass surface.

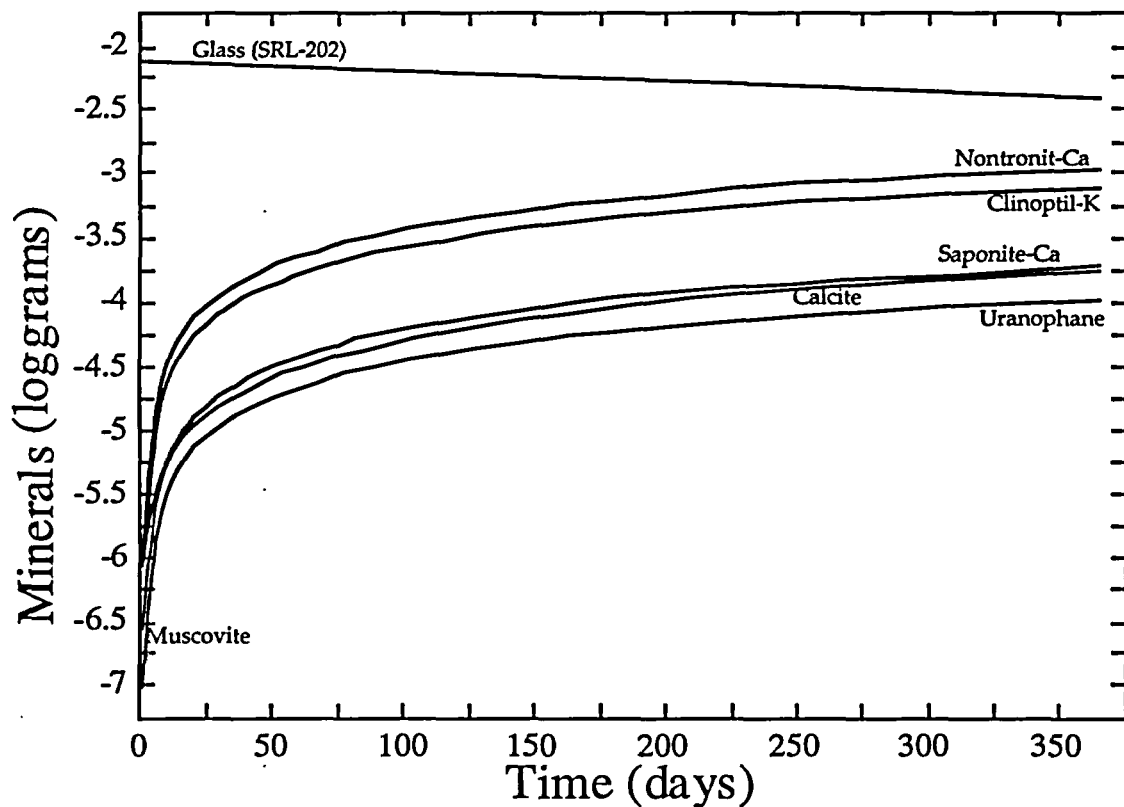


Figure 10. Secondary phases predicted to form by reaction of SRL-202 glass in EJ-13 water under unsaturated (drip) test conditions.

The model predicts that after one year, about 3.5 mg of glass will have reacted to form clays, zeolites, calcite, and uranophane (see Fig 10). The predicted extent of reaction and types of secondary phases are in good agreement with experimental results (Woodland, et al., 1991). The model also predicts the pH of the drop while on the glass surface will initially rise to a

value of about 9.25 from the starting pH of EJ-13 water of 7.8, and then fall with time to a value near 9 after one year (Fig. 11). This is caused by the glass surface becoming less reactive with time as the glass reacts with successive drops. Less reactive refers to the fact that the first few drops exhaust the ion exchange capacity of the glass surface; all the available alkalis are exchanged for hydronium ( $H_3O^+$ ) from solution. Note that the pH curve shown in Fig. 11 is the pH of the drop after it has reacted for 3.5 days prior to being displaced by the next drop. Fig. 12 shows the predicted elemental concentrations of species in the drop as a function of time. There is no way to compare these predictions with experimental data because the drop cannot be sampled while in contact with the glass surface. It may be possible to compare the integrated solution composition determined by adding up each predicted drop composition with the composition of the residual solution in the vessel bottom at the completion of the run. This has not yet been attempted.

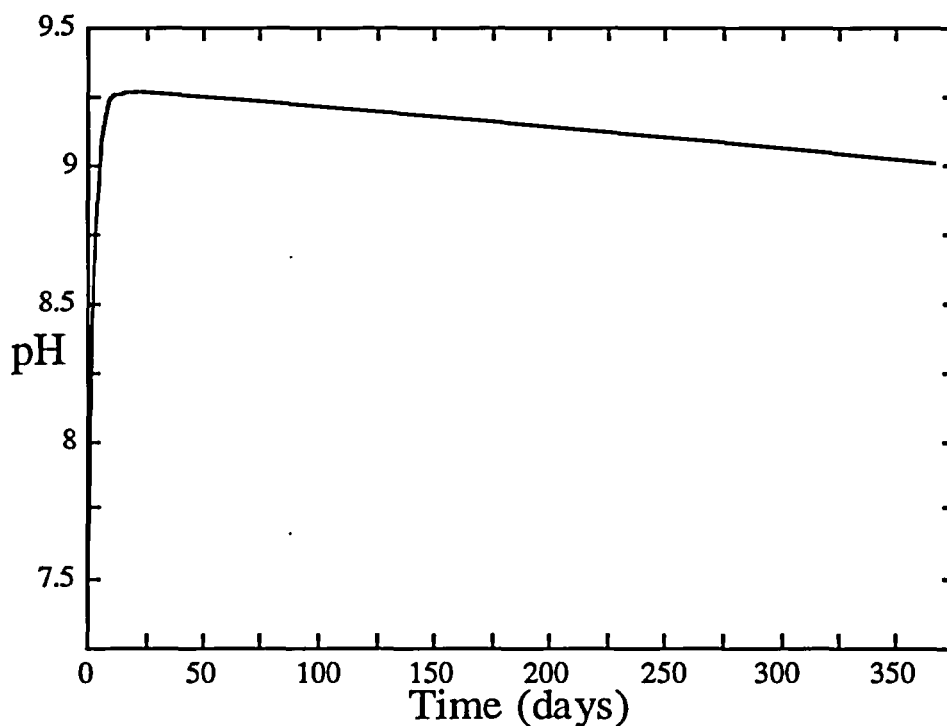


Figure 11. Predicted pH of drop while in contact with SRL-202 glass surface during unsaturated test (90°C pH).

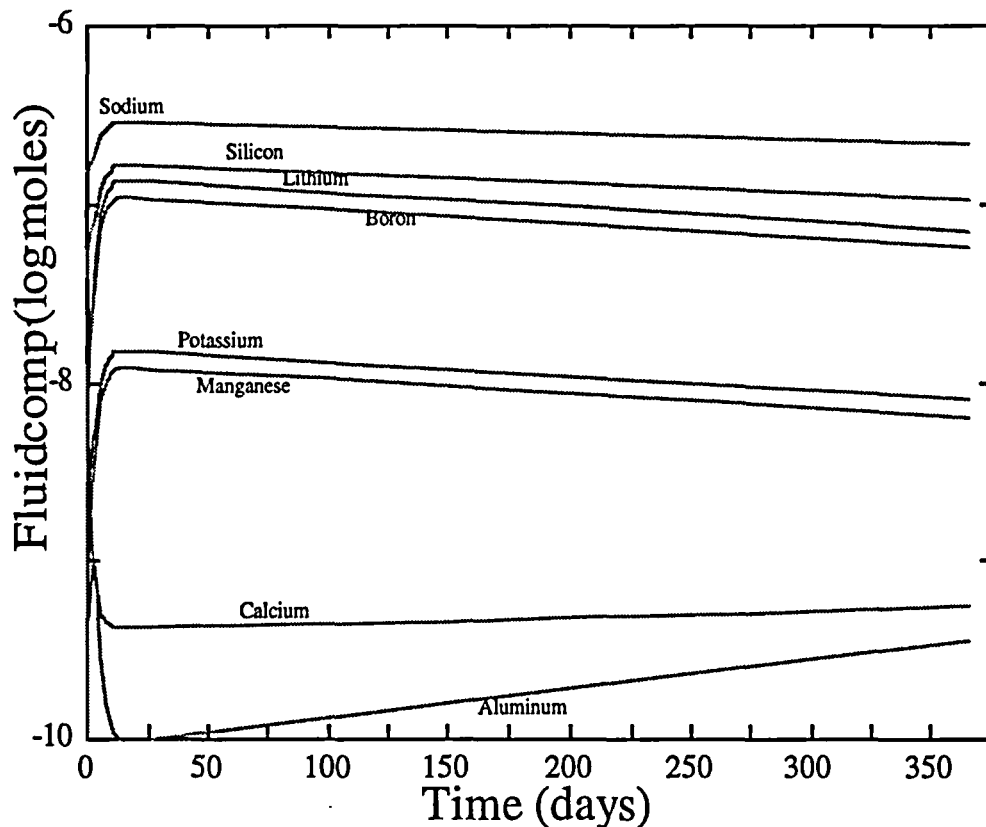


Figure 12. Predicted elemental composition of fluid phase (drop) while in contact with SRL-202 glass surface in unsaturated test.

### PART 3. IMPLICATIONS OF BORON CLUSTERING FOR MODELS OF GLASS COMPOSITION/DURABILITY

Previous work examining the local structure of borosilicate glasses using NMR spectroscopy (Bates, et al., 1994; Bates, et al., 1993) has shown that SRL-202 analog glasses are inhomogeneous on a length scale of a few tens of Angstroms. More soluble alkali-boron rich zones are present that very likely etch away faster than the silica-rich zones. Once etched out, these zones will provide permeable channel ways where water can more readily diffuse through and react with the glass. Glass dissolution rates will reflect these enhanced water diffusion rates when they are present. The channel ways effectively allow a greater surface area for contact between water and the glass.

In addition, boron and alkali release rates do not accurately reflect bulk glass dissolution rates, and must be corrected for the effect of the reduced durability of Na-B rich zones. In contrast, the boron-depleted residual groundmass effectively controls overall glass durability. The modified composition of this matrix material must be accounted for in order to

properly correlate glass composition with glass durability. For these reasons we believe an understanding of the fundamental glass structure is essential for proper interpretation of leach data, and NMR is the best technique for obtaining this information.

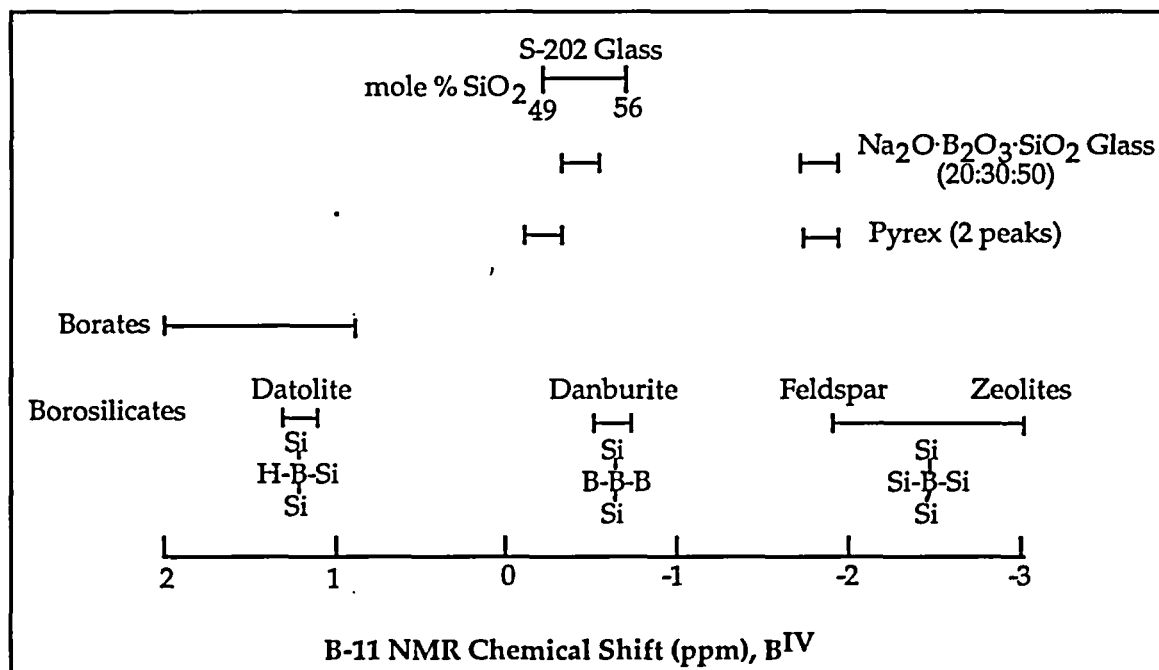


Figure 13. Range of NMR chemical shifts for 4-coordinated B in borates and borosilicates. Dashes in structural diagrams represent cation-oxygen-cation bonds.

#### Microscopic Structure of Borosilicate Glasses

The atomic-level structures for nine simple Na-borosilicate glasses were determined by NMR spectroscopic techniques (Bates, et al., 1994). The B-11 NMR data provide the population distribution of the various local boron structural units, including the ratio of three- to four-coordinated B (B<sup>3</sup>/B<sup>4</sup>). Correlation of this structural information with dissolution rates of the same samples allows us to develop detailed microscopic models for borosilicate glass dissolution. The study found that most of the boron present in the glass existed in boron-rich environments, i.e. most boron atoms had other boron atoms as next-nearest neighbors. Based on measured chemical shifts, the structural environment most closely matched that of the mineral danburite (CaB<sub>2</sub>(SiO<sub>4</sub>)<sub>2</sub> (see Fig. 13).

Information obtained from the Na-23 NMR data is only qualitative, but the NMR spectra were sensitive to whether the Na occur mostly in silicate or borate-like environments. The NaBS and S202 series gave non-overlapping ranges of Na-23 NMR peak position and opposing trends of peak position with varying silica content. These results can be interpreted in terms of the Na coordination number, consistent with current models of silicate glass structure. For the NaBS glasses, 70 to 85 percent of the Na are charge-balanced by B4, giving an average coordination number higher than in the S202 glasses, where that figure is less than 15 percent and most of the Na are charge-balanced by NBO's. Unfortunately, there is currently not enough Na-23 NMR data of model compounds available from which to construct a quantitative relationship between coordination number and NMR chemical shift.

Although the data are preliminary, the boron and sodium NMR data together indicate that the glass is clustered into regions of alkali-boron rich composition of an overall composition approximated by  $\text{Na}_2\text{B}_2(\text{SiO}_4)_2$  where the sodium in the formula may also represent lithium in lithium-containing glasses. Figure 14 shows the hypothetical local atomic structure.

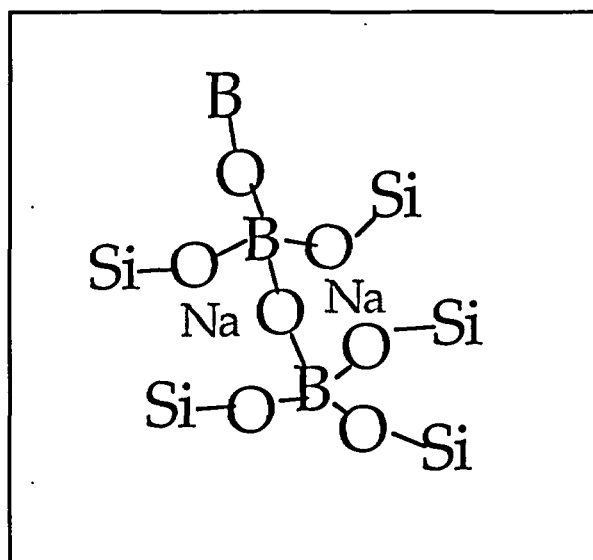


Figure 14. Hypothetical local atomic structure in boron-rich clusters of borosilicate glass, based on NMR data. The sodium atoms balance charge around four-coordinate boron and are more loosely bound to the structure than B and Si.

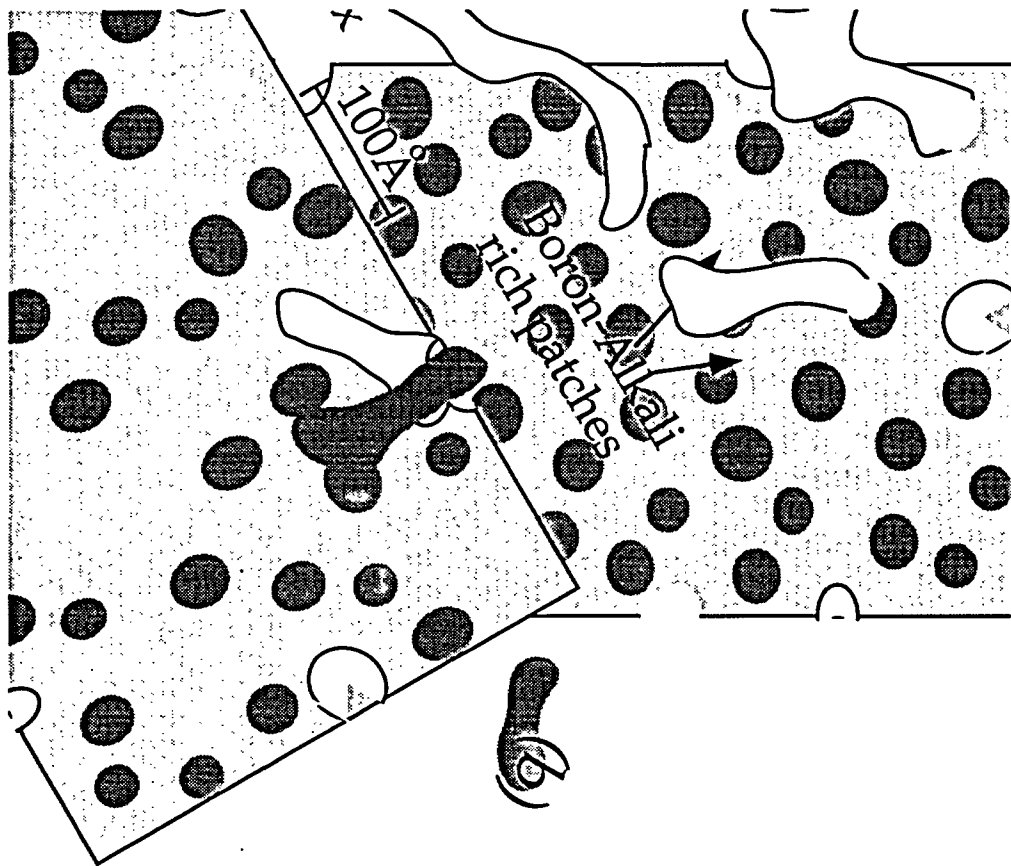


Figure 15. Schematic of borosilicate glass structure showing separation into boron-rich zones. (a) shows condition where zones are mainly segregated while (b) shows condition expected for more boron-rich glasses where coalescence gives rise to more elongated boron-rich zones. Type (b) glasses would have high effective surface areas (after soluble boron-rich zones are leached away) and transition between these two types of structures may be responsible for percolation-type transitions in glass durability.

## *Effect of Boron Clustering on Glass Composition-Durability Relationships*

A simple conceptual model can be used to account for the amounts of boron, alkali, and silicon present in the boron-rich clusters. In this model, the overall glass composition is modified to account for this phase separated material. This modified composition is then used in correlations of glass durability with glass composition. We assume here that the boron-rich regions are much more soluble than the silica-rich glass matrix (based on the high solubilities of most boron minerals including danburite). They will quickly dissolve away wherever they are in contact with the surface (see Fig. 15). As a consequence, more effective surface area contacts the solution and the overall dissolution rate increases proportionally to the exposed surface area.

In order to examine how great the change in matrix composition is due to clustering, we first use the SRL-202 composition expressed in terms of mole fraction of elements present (see Table 7). The amount of boron, sodium, and silicon present in the clusters is subtracted from the bulk composition. The amount of clustered material is limited by the amount of boron in the glass. We assume all the boron is present in the clusters. Thus, for each atom of boron present, one atom of sodium and one atom of silicon must be subtracted from the glass composition. Columns 4-7 of Table 7 show the results of this calculation for the SRL-202 glass composition. The relative amount of silica in the glass actually increases because of the reduced amounts of sodium and boron. Boron and sodium are reduced significantly. All of the other components increase in concentration by a small amount.

The important effect of this calculation is that the number of non-bridging oxygens (NBOs) calculated for the glass (15.3 mole % of alkalis; see Table 7) differs significantly from the number calculated for the uncorrected glass composition (17.5%). The number of NBOs calculated here is simply the number of moles of alkalis present minus the number of moles of trivalent cations. Glass durability is a strong function of the number of NBOs present in a glass. Non-bridging oxygens refer to the number of oxygen ions in the glass that are covalently bonded to only one cation. The network of Si-O-Si bonds in silica glasses is the primary structural feature that gives rise to their high durability in aqueous solutions. In order to predict glass durability from glass composition, it is critical to have an accurate evaluation of the number of NBOs present. The calculation shown here improves upon previous methods for estimating glass NBO content. We plan to extend this treatment to other glass compositions and re-evaluate the use of methods such as the "free energy of hydration" (Plodinec, et al., 1984), (Jantzen, 1992)) for correlating glass composition with glass durability. Better insight into this relationship will be used to guide the process of optimizing glass compositions for HLW disposal.

Table 7. SRL-202 composition renormalized to account for phase separation...

| Oxide  | Original Composition |           |            | Corrected for Phase Separation |           |          |
|--|----------------------|-----------|------------|--------------------------------|-----------|----------|
|  | Element              | oxide wt% | oxide mol% | oxide mol%                     | oxide wt% | cation%  |
| -  | -                    | -         | -          | -                              | -         | -        |
| SiO <sub>2</sub>                             | Si                   | 50.6781   | 56.3833    | 59.3449                        | 51.9319   | 44.2057  |
| Al <sub>2</sub> O <sub>3</sub>               | Al                   | 3.9756    | 2.6065     | 3.8158                         | 5.6664    | 5.6847   |
| B <sub>2</sub> O <sub>3</sub>                | B                    | 8.2514    | 7.9231     | 0.0000                         | 0.0000    | 0.0000   |
| Mn <sub>2</sub> O <sub>3</sub>               | Mn                   | 2.2777    | 0.9644     | 1.4119                         | 3.2464    | 2.1034   |
| Fe <sub>2</sub> O <sub>3</sub>               | Fe                   | 11.8128   | 4.9449     | 7.2392                         | 16.8370   | 10.7849  |
| Na <sub>2</sub> O                            | Na                   | 9.2349    | 9.9605     | 2.9826                         | 2.6924    | 4.4435   |
| K <sub>2</sub> O                             | K                    | 3.8410    | 2.7258     | 3.9905                         | 5.4746    | 5.9450   |
| Li <sub>2</sub> O                            | Li                   | 4.3793    | 9.7971     | 14.3426                        | 6.2419    | 21.3675  |
| CaO  | Ca                   | 1.2424    | 1.4809     | 2.1680                         | 1.7708    | 1.6150   |
| MgO  | Mg                   | 1.3666    | 2.2666     | 3.3183                         | 1.9478    | 2.4718   |
| U <sub>3</sub> O <sub>8</sub>                | U                    | 1.9981    | 0.1586     | 0.2322                         | 2.8480    | 0.5189   |
| TiO <sub>2</sub>                             | Ti                   | 0.9421    | 0.7882     | 1.1540                         | 1.3428    | 0.8596   |
| Totals                                       |                      | 100.0000  | 100.0000   | 100.0000                       | 100.0000  | 100.0000 |
| Non-bridging Oxygens = 15.3 mole% of cations |                      |           |            |                                |           |          |

## REFERENCES

- Bates, J. K., Bourcier, W. L., Bradley, C. R., Brown, N. R., Buck, E. C., Carroll, S. A., Cunnane, J. C., Dietz, N. L., Gerding, T. J., Gong, M., Hafenrichter, L. D., Hoh, J. C., Mazer, J. C., Newton, L., Phillips, B. L., Pletcher, R., and Wronkiewicz, D. J. (1994). ANL Technical Support Program of DOE Environmental Restoration and Waste Management Report No. ANL-94/19. Argonne National Laboratory.
- Bates, J. K., Bourcier, W. L., Bradley, C. R., Buck, E. C., Cunnane, J. C., Dietz, N. L., Ebert, W. L., Emery, J. W., Ewing, R. C., Feng, X., Gerding, T. J., Gong, M., Hoh, J. C., Li, H., Mazer, J. J., Morgan, L. E., Newton, L., Nielsen, J. K., Phillips, B. L., Tomozawa, M., Wang, L. M., and Wronkiewicz, D. J. (1993). ANL Technical Support Program for DOE Environmental Restoration and Waste Management; Annual Report, October 1991-September 1992 No. ANL-93/13. Argonne National Laboratory.
- Bates, J. K., and Gerding, T. J. (1989). NNWSI waste form test method for unsaturated disposal conditions No. UCRL-15723. Lawrence Livermore National Laboratory.
- Baxter, R. G. (1983). Description of defense waste processing facility reference waste form and container. Report No. Dp-1606. Savannah River Plant.

- Bethke, C. M. (1992). The Geochemist's Workbench: A users guide to Rxn, Act2, Tact, React, and Gtplot. U. of Illinois Press.
- Bourcier, W. L. (1994). Critical review of glass performance modeling Report No. ANL-94/17. Argonne National Laboratory.
- Cunnane, J. C. e. (1993). High-level waste borosilicate glass: a compendium of corrosion characteristics. No. DOE-EM-0177. DOE-EM-0177USDOE Office of Waste Management.
- Delage, F., Ghaleb, D., Dussossoy, J. L., Chevallier, O., and Vernaz, E. (1992). A mechanistic model for understanding nuclear waste. *J. Nuc. Materials*, **190**:191-197.
- Jantzen, C. M. (1992). Thermodynamic approach to glass corrosion. In D. E. Clark & B. K. Zoitos (Eds.), Corrosion of Glass, Ceramics, and Ceramic Superconductors (pp. 153-215). Park Ridge, New Jersey: Noyes Publications.
- Johnson, J. W., Oelkers, E. H., and Helgeson, H. C. (1992). SUPCRT92: A software package for calculating the standard molal thermodynamic properties of minerals, gases, aqueous species, and reactions from 1 to 5000 g=bars and 0 to 1000C. *Computers and Geosciences*, **18**:890-947.
- Knauss, K. G., Beiringer, W. J., and Peifer, D. W. (1987). Hydrothermal interaction of solid wafers of Topopah Spring Tuff with J-13 water at 90 and 150C using Dickson-type gold bag rocking autoclaves: Long-term experiments. Report No. UCRL-53722. Lawrence Livermore National Laboratory.
- Knauss, K. G., Bourcier, W. L., McKeegan, K. D., Merzbacher, C. I., Nguyen, S. N., Ryerson, F. J., Smith, D. K., Weed, H. C., and Newton, L. (1990). Dissolution kinetics of a simple nuclear waste glass as a function of pH, time, and temperature. *Mat. Res. Soc. Symp. Proc.*, **176**:371-381.
- Lamont, A. D., and Gansemer, J. D. (1994). User guide to the Yucca Mountain Integrating Model (YMIM), version 2.1. Report No. UCRL-LR-116446. Lawrence Livermore National Laboratory.
- Plodinec, M. J., Jantzen, C. M., and Wicks, G. G. (1984). Stability of radioactive waste glasses assessed from hydration thermodynamics. *Mat. Res. Soc. Symp. Proc.*, **26**:755-762.
- Stout, R. B., and Leider, H. R. (1991). Preliminary Waste Form Characteristics Report Version 1.0 Report UCRL-ID-108314 Rev. 1. Lawrence Livermore National Laboratory.
- Wilder, D. G. ed. (1992). Near-field environment report volume I: Technical basis for BES design No. UCRL-LR-107476. Lawrence Livermore National Laboratory.
- Wolery, T. J. (1992). EO3/6, A software package for geochemical modeling of aqueous systems: Package overview and installation guide. No. UCRL-MA-110662 PT 1. Lawrence Livermore National Laboratory.

Woodland, A. B., Bates, J. K., and Gerding, T. J. (1991). Parametric effects on glass reaction in the unsaturated test method. No. ANL-91/36. Argonne National Laboratory.